IARJSET ISSN (O) 2393-8021, ISSN (P) 2394-1588

International Advanced Research Journal in Science, Engineering and Technology

Impact Factor 8.311 ⁜ Peer-reviewed & Refereed journal ⁜ Vol. 12, Issue 8, August 2025

DOI: 10.17148/IARJSET.2025.12808

Similarity Solutions for Natural Convection Flow and Heat Transfer of Powell-Eyring Fluids in Porous Media with Heat Source Effects

Patil S.K[1], Sonawane P.M[2]

Department of Mathematics, Moolji Jaitha College (Autonomous), Jalgaon, Dist. Jalgaon, India[1]

Department of Mathematics, Dhanaji Nana Mahavidyalaya, Faizpur, Dist. Jalgaon, India[2]

Abstract: This study investigates the natural convection flow and heat transfer characteristics of Powell–Eyring non-Newtonian fluids in a porous medium, incorporating the effects of internal heat generation or absorption. The governing equations—continuity, momentum, and energy—are formulated for an incompressible, laminar flow regime and transformed into a dimensionless form using similarity variables derived through group symmetry analysis. The Powell–Eyring constitutive relation introduces non-linear rheological behavior, transitioning smoothly to Newtonian fluid behavior under specific parameter limits. The resulting coupled non-linear ordinary differential equations are solved numerically using established methods such as the Runge–Kutta shooting technique. Parametric analyses are performed to assess the influence of key dimensionless parameters, including the Prandtl number, porous drag coefficient, heat source/sink strength, and Powell–Eyring fluid constants, on velocity and temperature profiles. The findings provide insights into thermal boundary layer behavior in complex rheological fluids and are applicable to engineering systems involving porous media heat transfer, such as geothermal reservoirs, polymer processing, and energy storage devices.

Keywords: Natural convection; Powell–Eyring fluid; Porous media; Heat source/sink; Similarity transformation; Non-Newtonian fluids; Boundary layer theory; Numerical solution.

I. INTRODUCTION

Natural convection in porous media has wide-ranging applications in engineering and geophysical systems, including cooling of electronic components, geothermal energy extraction, and filtration processes. The study of such flows becomes more challenging when the working fluid exhibits non-Newtonian characteristics, as is the case with Powell–Eyring fluids, which display shear-thinning or shear-thickening behavior depending on operational conditions. The Powell–Eyring model captures these complex rheological features through an inverse hyperbolic sine relation in the constitutive equation, providing a more accurate description of polymeric and suspension flows compared to purely Newtonian models. In the presence of porous structures, additional resistance due to the matrix affects the fluid motion, while internal heat generation or absorption further modifies the thermal field. Group similarity transformation techniques offer an elegant approach to reducing the governing partial differential equations into a tractable system of ordinary differential equations. These methods facilitate the identification of scaling laws and the parametric influences on flow and heat transfer behavior. The present work applies this methodology to derive similarity solutions for the coupled momentum and energy equations governing the natural convection of Powell–Eyring fluids in porous media, under the influence of a uniform heat source or sink.

Lee and Amen (1966) focused on reducing the governing boundary-layer equations into dimensionless forms using similarity variables, thereby facilitating analytical and semi-analytical solutions. This pioneering study provided the theoretical foundation for later developments in similarity transformation techniques for non-Newtonian flow problems. **Timol and Kalthia (1990)** systematically identified similarity variables using Lie group symmetry analysis, reducing the partial differential equations into solvable ordinary differential equations. This method significantly influenced later studies by enabling generalized analytical formulations for different classes of non-Newtonian fluids. **Mukhopadhyay et al. (2005)** demonstrated the combined effects of magnetic fields and variable viscosity on velocity and temperature distributions, highlighting the importance of these parameters in controlling heat transfer rates. This work bridged the gap between pure fluid mechanics and electromagnetic effects in thermal boundary-layer theory. **Mukhopadhyay et al. (2012)** incorporated radiation heat transfer into the momentum and energy equations and examined its influence on velocity and temperature fields. Their findings emphasized the significance of porous drag and radiative heat flux in modifying boundary-layer thickness and overall thermal performance. **Hayat et al. (2013)** obtained self-similar

IARJSET ISSN (O) 2393-8021, ISSN (P) 2394-1588

International Advanced Research Journal in Science, Engineering and Technology

Impact Factor 8.311 ⁜ Peer-reviewed & Refereed journal ⁜ Vol. 12, Issue 8, August 2025

DOI: 10.17148/IARJSET.2025.12808

solutions and discussed the influence of non-Newtonian parameters on velocity and temperature profiles. Their study highlighted the sensitivity of the thermal boundary layer to variations in fluid elasticity and stretching rates. **Sonawane et al. (2016)** demonstrated how fluid elasticity and power-law index affect natural convection characteristics in vertical channels. The study provided practical insights for industrial processes involving non-linear rheological fluids. **Darji and Timol. (2016)** derived exact similarity solutions for various rheological models. Their results underscored the adaptability of group-theoretic methods for a wide range of non-Newtonian heat transfer problems. **Patel et al. (2017)** examined the effects of flow parameters such as Prandtl number and fluid elasticity on velocity and temperature fields, demonstrating how non-linear fluid behavior can be systematically analyzed using symmetry methods. **Ferdows et al. (2020)** incorporated buoyancy effects and stratification into the similarity framework, revealing that thermal stratification significantly modifies the heat transfer rate by altering temperature gradients near the wall. **Mansour et al. (2021)** showed that magnetic fields, nanoparticle concentration, and geometric configuration strongly influence heat transfer enhancement. This work extended classical natural convection theory to modern nanofluid applications.

II. GOVERNING EQUATIONS

Continuity:

$$\frac{\partial u}{\partial x}+\frac{\partial v}{\partial y}=0 \tag{1}$$

Ensures mass conservation for incompressible flow.

Momentum (x-direction):

$$u\frac{\partial u}{\partial x}+v\frac{\partial u}{\partial y}=g\beta(T-T_\infty)+\frac{1}{\rho}\frac{\partial \tau_{xy}}{\partial y}-\frac{\mu}{K}u \tag{2}$$

$u\frac{\partial u}{\partial x}+v\frac{\partial u}{\partial y}$: Convective acceleration.

Buoyancy term $g\beta(T-T_\infty)$ promotes upward motion for heated fluid.

Shear stress gradient $\frac{\partial \tau_{xy}}{\partial y}$ depends on the chosen non-Newtonian model.

Porous drag term $\frac{\mu}{K}u$ reduces flow due to matrix resistance.

Energy:

$$u\frac{\partial T}{\partial x}+v\frac{\partial T}{\partial y}=\alpha\frac{\partial^2 T}{\partial y^2}+\frac{Q}{\rho C_p}(T-T_\infty) \tag{3}$$

Captures convective heat transfer (LHS) balanced with thermal diffusion and internal generation (RHS).

$\boldsymbol{Q}$ introduces uniform heat generation or absorption.

III. CONSTITUTIVE RELATION

These define$\boldsymbol{\tau_{xy}}$, the shear stress, essential for characterizing the non-linear behaviour of fluids:

Powell-Eyring:

$$\tau_{xy}=\mu\frac{\partial u}{\partial y}\left[1-\frac{1}{sinh^{-1}\left(\in\frac{\partial u}{\partial y}\right)}\right] \tag{4}$$

Non-linear dependence due to inverse hyperbolic sine term.

Behaviour transitions to Newtonian when $\in\rightarrow 0$.

IARJSET ISSN (O) 2393-8021, ISSN (P) 2394-1588

International Advanced Research Journal in Science, Engineering and Technology

Impact Factor 8.311 ⁜ Peer-reviewed & Refereed journal ⁜ Vol. 12, Issue 8, August 2025

DOI: 10.17148/IARJSET.2025.12808

Boundary Condition:

At $y = 0$: $u = 0, \quad v = 0, \quad T = T_W$

As $y \to \infty$: $u \to 0, \quad T \to T_\infty$

IV. INTRODUCED DIMENSIONLESS VARIABLES

Let

$x = Lx^*$, $y = Ly^*$ (spatial scaling) (5)

$u = U_0 u^*$, $v = U_0 u^*$ (flow velocity scaling)

$T = T^* \Delta T + T_\infty$ (temperature scaling, where ΔT characteristic temperature difference)

$\tau_{xy} = \frac{\mu U_0}{L} \tau^*_{xy}$

Using equation (4) equation (1), (2) and (3) becomes

$$\frac{\partial u^*}{\partial x^*} + \frac{\partial v^*}{\partial y^*} = 0 \quad (6)$$

$$u^* \frac{\partial u^*}{\partial x^*} + v^* \frac{\partial u^*}{\partial y^*} = G_r T^* + \frac{1}{R_e} \frac{\partial \tau^*_{xy}}{\partial y^*} - \frac{1}{D_a R_e} u^* \quad (7)$$

$$u^* \frac{\partial T^*}{\partial x^*} + v^* \frac{\partial T^*}{\partial y^*} = \frac{1}{P_e} \frac{\partial^2 T^*}{\partial y^{*2}} + ST \quad (8)$$

Where:

$G_r = \frac{g \beta \Delta T L^3}{V^2}$

$R_e = \frac{\rho U_0 L}{\mu}$

$D_a = \frac{K}{L^2}$

$P_e = \frac{U_0 L}{\alpha}$

$S = \frac{QL}{\rho c_p U_0}$

Non-dimensional parameters

$$u^* = \frac{\partial \psi^*}{\partial y^*}, v^* = -\frac{\partial \psi^*}{\partial x^*} \quad (9)$$

Stream function automatically satisfies continuity equation, equation (6) & (7) becomes

$$\psi^*_y - \psi^*_{xy} - \psi^*_x - \psi^*_{yy} = G_r T^* + \frac{1}{R_e} \frac{d}{dy^*} \left[\psi^*_{yy} \left(1 - \frac{1}{\epsilon^* sinh^{-1}(\epsilon \psi_{yy})} \right) \right] - \frac{1}{D_a R_e} \psi^*_y \quad (10)$$

$$\psi^*_x T^*_x - \psi^*_x T^*_y = \frac{1}{P_e} T^*_{yy} + ST^* \quad (11)$$

IARJSET ISSN (O) 2393-8021, ISSN (P) 2394-1588

International Advanced Research Journal in Science, Engineering and Technology

Impact Factor 8.311 ⁜ Peer-reviewed & Refereed journal ⁜ Vol. 12, Issue 8, August 2025

DOI: 10.17148/IARJSET.2025.12808

At $y^* = 0$: $\psi^* = 0,\ \psi_y^* = 0,\ T^* = 1$

As$y^* \to \infty$: $\psi_y^* \to 0,\ T^* \to 0$

V. GROUP SIMILARITY VARIABLES

To reduce the PDE system into ODEs:

$$\eta = y^* x^{*^{-a}}, \psi^*(x^* y^*) = x^{*^b} f(\eta), T^*(x^* y^*) = \theta(\eta) \quad (12)$$

Transforms the 2D boundary-layer equations into a system of coupled nonlinear ODEs with respect to similarity variable η.

1) **6.** Transformed ODE System:

(i) Momentum Equation

Powell-Eyring:

$$ff'' - (f')^2 = G_r\theta + \frac{1}{R_e}\frac{d}{d\eta}\left[f''\left(1 - \frac{1}{\epsilon^* sinh^{-1}(\epsilon f'')}\right)\right] - \frac{1}{D_a R_e} f' \quad (13)$$

Energy Equation:

$$f\theta' = \frac{1}{P_e}\theta'' + S\theta \quad (14)$$

Prandtl number (Pr)governs thermal boundary layer.

S acts as a source/sink strength parameter, changing the profile of θ.

Boundary Conditions:

At $\eta = 0$: $f(0) = 0,\quad f'(0) = 0,\quad \theta(0) = 1$

As$\eta \to \infty$: $f'(\infty) \to 0,\quad \theta(\infty) \to 0$

VI. SOLUTION APPROACH

To solve numerically (e.g., with Runge-Kutta), reduce the system to first-order ODEs**.** Introduce new variables:

$$f = y_1, f' = y_2, f'' = y_3, \theta = y_4, \theta' = y_5 \quad (15)$$

Then the system becomes:

System for Powell–Eyring Fluid

$$\frac{dy_1}{d\eta} = y_2 \quad (16)$$

$$\frac{dy_2}{d\eta} = y_3 \quad (17)$$

$$\frac{dy_3}{d\eta} = \frac{y_1 y_3 - y_2^2 - G_r y_4 + \frac{1}{D_a R_e} y_2}{\frac{1}{R_e}\left(1 - \frac{1}{\epsilon^* sinh^{-1}(\epsilon f''')}\right)} \quad (18)$$

$$\frac{dy_4}{d\eta} = y_5 \quad (19)$$

$$\frac{dy_5}{d\eta} = P_e(y_1 y_5 - S y_4) \quad (20)$$

Boundary Conditions in New Variables

$$y_1(0) = f(0) = 0$$

IARJSET ISSN (O) 2393-8021, ISSN (P) 2394-1588

International Advanced Research Journal in Science, Engineering and Technology

Impact Factor 8.311 ⁜ Peer-reviewed & Refereed journal ⁜ Vol. 12, Issue 8, August 2025

DOI: 10.17148/IARJSET.2025.12808

$y_2(0) = f'(0) = 0$
$y_4(0) = \theta(0) = 1$
$y_2(\infty) = f'(\infty) = 0$
$y_4(\infty) = \theta(\infty) = 0$

VII. RESULTS AND DISCUSSION

Graph 1: Temperature profiles vs Prandtl number (S=0)

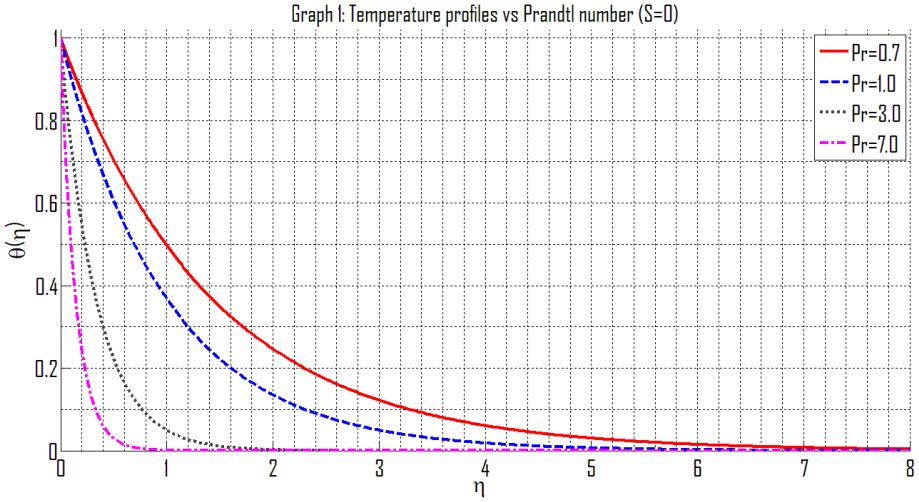

Graph 2: Temperature profiles vs heat source/sink S (Pr=1.0)

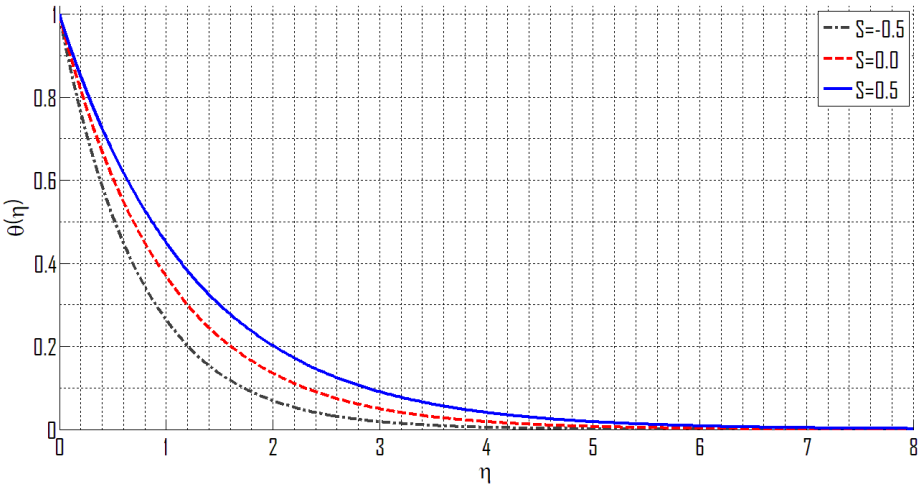

Graph 3: Thermal layer thickness vs Pr for different S

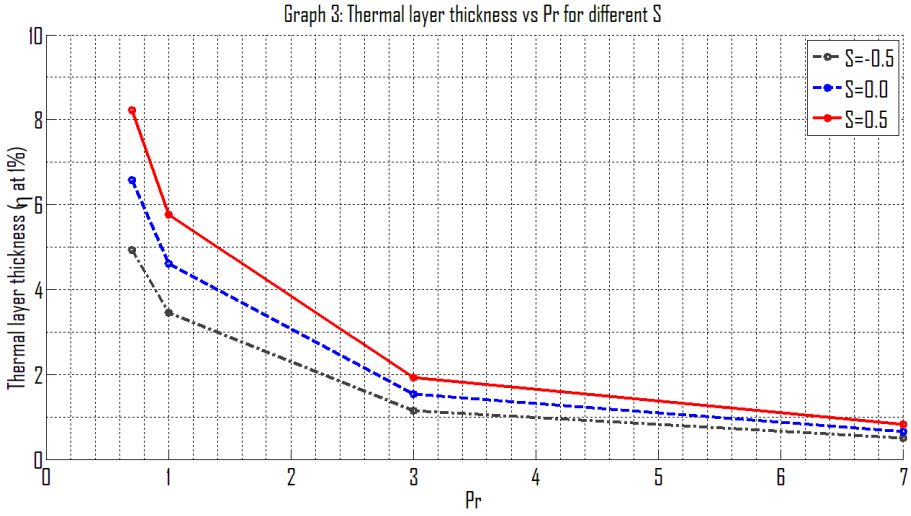

IARJSET ISSN (O) 2393-8021, ISSN (P) 2394-1588

International Advanced Research Journal in Science, Engineering and Technology

Impact Factor 8.311 ⁜ Peer-reviewed & Refereed journal ⁜ Vol. 12, Issue 8, August 2025

DOI: 10.17148/IARJSET.2025.12808

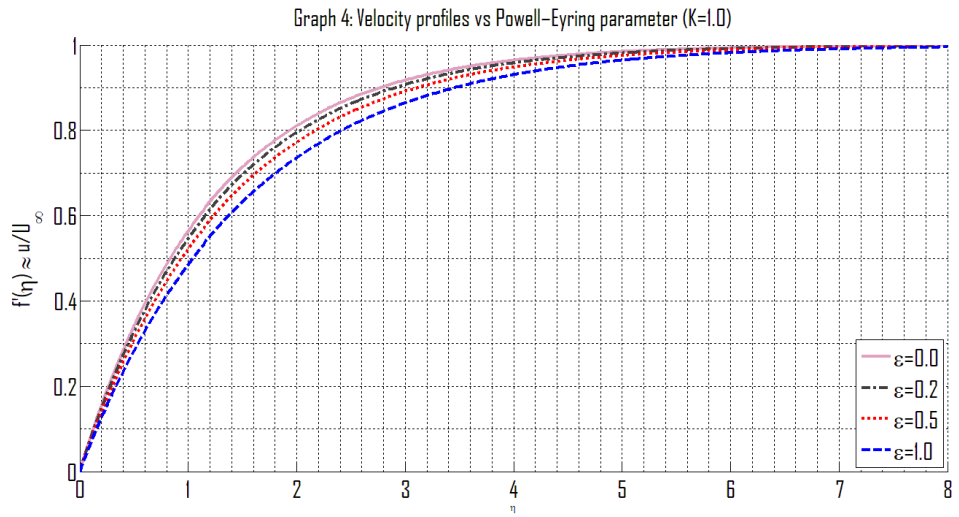

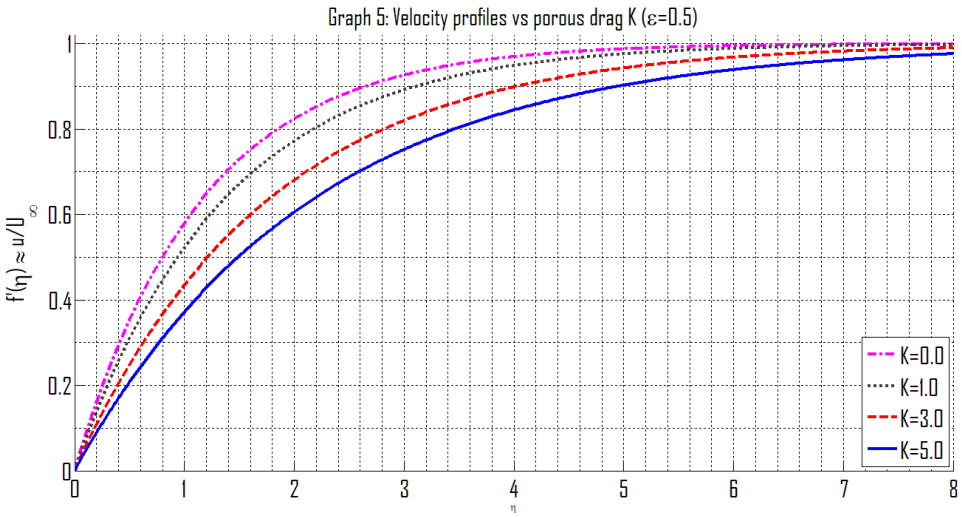

The graph (1) depicts the variation of the dimensionless temperature profile θ(η) with the similarity variable η for different Prandtl numbers (Pr=0.7,1.0,3.0,) in the absence of a heat source/sink (S=0). It shows that as the Prandtl number increases, the thermal boundary layer becomes thinner and the temperature decays more rapidly away from the wall. For lower Prandtl numbers (e.g., Pr=0.7), heat diffuses more quickly relative to momentum, resulting in a thicker thermal boundary layer and a slower decay of temperature. Conversely, for higher Prandtl numbers (e.g., Pr=7.0), heat conduction is weaker compared to momentum diffusion, leading to a sharper drop in temperature close to the wall. This behavior is consistent with the physical meaning of the Prandtl number, where higher values indicate fluids with lower thermal diffusivity.

The graph (2) illustrates the influence of the heat source/sink parameter S on the dimensionless temperature profile θ(η) for a fixed Prandtl number (Pr=1.0). When S>0 (e.g., S=0.5, blue curve), representing a heat source, the temperature remains higher throughout the boundary layer and decays more slowly with η, indicating a thicker thermal boundary layer due to additional heat generation. For S=0 (red dashed line), representing no heat source or sink, the temperature decay follows a baseline profile. When S<0 (e.g., S=−0.5, black dash-dotted line), representing a heat sink, the temperature decreases more rapidly with η, resulting in a thinner thermal boundary layer as heat is removed from the fluid. This trend clearly shows that a heat source enhances temperature distribution, whereas a heat sink suppresses it.

The graph (3) presents the variation of thermal layer thickness δ_t (evaluated at 1% of the wall temperature) with the Prandtl number (Pr) for different heat source/sink values (S=−0.5,0.0,0.5). Across all cases, δ_t decreases sharply as Pr increases, indicating that higher Prandtl numbers correspond to thinner thermal boundary layers due to reduced thermal diffusivity. For a given Pr, the presence of a heat source (S=0.5, red curve) leads to the largest δ_t , as additional heat generation increases the temperature penetration into the fluid. The baseline case (S=0.0, blue curve) lies between the two extremes. In contrast, a heat sink (S=−0.5, black curve) produces the thinnest thermal layer, as heat removal

IARJSET ISSN (O) 2393-8021, ISSN (P) 2394-1588

International Advanced Research Journal in Science, Engineering and Technology

Impact Factor 8.311 ⁜ Peer-reviewed & Refereed journal ⁜ Vol. 12, Issue 8, August 2025

DOI: 10.17148/IARJSET.2025.12808

suppresses temperature diffusion away from the wall. The gap between the curves is most pronounced at low Pr and narrows at higher Pr, showing that heat source/sink effects are more significant in fluids with higher thermal diffusivity.

The graph (4) illustrates the effect of the Powell–Eyring fluid parameter ε\varepsilonε on the dimensionless velocity profile $f'(\eta) \approx \frac{u}{U_\infty}$ for a fixed porous medium parameter (K=1.0). As ε\varepsilonε increases from 0.0 to 1.0, the velocity profile rises more gradually near the wall and approaches the free-stream velocity at a slightly larger η. This indicates that higher ε values, representing stronger non-Newtonian effects in the Powell–Eyring model, tend to reduce the velocity gradient at the wall and slightly thicken the momentum boundary layer. For ε=0.0, the behavior corresponds to a Newtonian fluid, exhibiting the steepest initial velocity rise. The differences among profiles are more noticeable close to the wall region (η<2) and diminish farther from it, where all curves converge to the free-stream value.

The graph (5) shows the influence of the porous drag parameter K on the dimensionless velocity profile $f'(\eta) \approx \frac{u}{U_\infty}$ for a Powell–Eyring fluid with ε=0.5. As K increases from 0.0 to 5.0, the velocity profiles become noticeably flatter near the wall and rise more gradually toward the free-stream value. This behavior reflects the enhanced resistance offered by the porous medium: higher K values correspond to greater drag, which suppresses fluid motion and thickens the momentum boundary layer. For K=0.0 (no porous resistance), the velocity increases rapidly from the wall and reaches the free-stream value more quickly, indicating a thinner boundary layer. The effect of K is most significant within the near-wall region (η<3) and diminishes farther away, where all profiles eventually converge to unity.

VIII. CONCLUDING REMARKS

The similarity transformation approach effectively reduces the governing equations for Powell–Eyring fluid flow in a porous medium to a coupled set of non-linear ordinary differential equations, enabling efficient numerical analysis. The results highlight the significant influence of fluid rheology, porous drag, and heat generation/absorption on velocity and temperature distributions. Specifically:

(i) Increasing the non-Newtonian parameters alters the velocity gradient near the wall and modifies the thickness of the thermal boundary layer.

(ii) Heat source effects elevate temperature profiles, while heat sinks reduce them, directly impacting the convective heat transfer rate.

(iii) The porous medium's resistance dampens fluid motion, leading to steeper thermal gradients.

(iv) Prandtl number variations significantly influence the thermal layer thickness, with higher values reducing heat diffusion.

These findings are relevant to the design and optimization of systems where controlling heat transfer in non-Newtonian porous flows is critical. Future studies could extend this work to include transient effects, anisotropic porous media, and magnetohydrodynamic influences for broader applicability.

REFERENCES

[1]. Darji R.M., Timol M.G. (2016): "Generalized non-Newtonian fluid flow analysis of heat transfer in natural convection – A deductive group symmetry approach", *International Journal of Advanced Applied Mathematics and Mechanics*, 4(1): 11–20.

[2]. Ferdows M., Bhuiyan M.M., Alam M.S., Siddiqa M.S. (2020): "Flow and heat transfer analysis of Eyring–Powell fluid over stratified sheet with mixed convection", *Journal of Engineering and Applied Science*, (2020).

[3]. Hayat T., Ali S., Alsaedi A. (2013): "Self-similar solutions for the flow and heat transfer of Powell–Eyring fluid over a non-isothermal stretching sheet", *International Journal of Heat and Mass Transfer*, 65: 251–258.

[4]. Lee S.Y., Amen W.F. (1966): "Similar solutions for non-Newtonian fluids", *AIChE Journal*, 12: 700–708.

[5]. Mansour M.A., Gorla R.S., Siddiqa S., Rashad A.M., Salah T. (2021): "Unsteady MHD natural convection flow of a nanofluid inside an inclined square cavity containing a heated circular obstacle", *International Journal of Thermal Sciences*, (Published online June 9, 2021).

IARJSET ISSN (O) 2393-8021, ISSN (P) 2394-1588

International Advanced Research Journal in Science, Engineering and Technology

Impact Factor 8.311 ⁜ Peer-reviewed & Refereed journal ⁜ Vol. 12, Issue 8, August 2025

DOI: 10.17148/IARJSET.2025.12808

[6]. Mukhopadhyay S., De P.R., Bhattacharyya K., Layek G.C. (2012): "Forced convective flow and heat transfer over a porous plate in a Darcy–Forchheimer porous medium in presence of radiation", *Meccanica*, 47(1): 153–161.

[7]. Mukhopadhyay S., Layek G.C., Samad S.A. (2005): "Study of MHD boundary layer flow over a heated stretching sheet with variable viscosity", *International Journal of Heat and Mass Transfer*, 48(21–22): 4460–4466.

[8]. Patel Manisha, Darji R., Timol M.G. (2017): "Similarity solution of forced convection flow of Powell–Eyring, Prandtl–Eyring fluids by group-theoretic method", *Mathematical Journal of Interdisciplinary Sciences*, 5(2): 45–60.

[9]. Sonawane P., Timol M.G. Salunke J.N. (2016): "Similarity Solution of Laminar Natural Convection Flow of Non-Newtonian Visco inelastic Fluids", *International Journal of Innovative Science*, *Engineering and Technology*, 3(7): 194-201.

[10]. Timol M.G., Kalthia N.L. (1990): "Group theoretic approach to similarity solutions in non-Newtonian natural convection flows", *Regional Journal of Energy Heat and Mass Transfer*, 7(4): 251–288.

